International Journal of Multiphysics
Volume 19, No. 1, 2025
ISSN: 1750-9548

On the Implementation of the Eco-Friendly Geopolymer Concrete Incorporating Autoclaved Aerated Block Waste Aggregate; Experimental Assesment and AI Modeling

Seyed Ali Taleghani-esfahani[1], Mohammadhossein Mahmoudisari [2]*, Majid Safehian[3]

1- Department of Civil Engineering, SR.C., Islamic Azad University, Tehran, Iran

2- Faculty of Architecture and urban design, University of Art, Tehran, Iran (Mahmoudi@art.ac.ir)

3- Department of Civil Engineering, SR.C., Islamic Azad University, Tehran, Iran

Abstract

Geopolymer mixtures offer an enhanced alternative to implement an eco-friendly solution in construction industry. These mixtures exhibit similar or better mechanical and structural properties in comprising of cement and can use recycling and by-product materials. Against this background, an eco-friendly advantageous were achieved from the engineers and researchers by using waste materials to replace cement and attention to reduce CO_2 emission during its procedure. Therefore, an eco-friendly geopolymer concrete (GPC) incorporating autoclaved aerated block waste (AABW) aggregate with Na_2SiO_3 / NaOH =1/5 and molarity=12 were developed. Moreover, the geopolymer mixtures were exposed to elevated temperature between 200 and 800 ^{0}C. Then, the post-fire evaluation, mechanical behaviour and micro structure analysis were investigated. The proposed research presented that the fibers slightly decreased the compressive strength of GPC and the 1.25% PP fibres displayed the least performance, i.e. around 13% decrease, compared to the unreinforced mixtures. Post-fire behaviour of mixtures exhibit that the compressive strength of eco-friendly GPC containing AABW aggregate increased first for all mixes but in the range of 400 - 800°C it decreased at a higher rate due to the dehydration of the geopolymer matrix. Besides, the melting of the fibres due to high temperature and the thermal reaction mechanism of free water evaporation causes the reduction on mechanical properties by a temperature range of 400°C to 800°C. At the second step, the machine learning techniques (e.g., multilayer perceptron neural network and M5 prime) were used for modeling of the compressive, tensile strength and module of elasticity of eco-friendly GPC containing AABW aggregate.

Keywords: Eco-friendly concrete, autoclaved aerated block waste aggregate, post-fire behaviour, mechanical properties, machine learning.

1. Introduction

Portland cement concrete (PCC) is one of the most extensively utilized construction materials due to its high compressive strength, durability, and versatility. The primary binder in PCC is Ordinary Portland Cement (OPC), which typically comprises 10–15% of the total concrete mass. The remaining constituents include fine aggregates (sand), coarse aggregates (gravel or crushed stone), water, and, in some cases, supplementary cementitious materials (SCMs) or chemical admixtures to enhance specific properties. Despite its widespread application, OPC production poses significant environmental challenges. The manufacturing process, which involves calcination of limestone at high temperatures in rotary kilns, is energy-intensive and releases substantial amounts of carbon dioxide (CO_2) [1]. It is estimated that for every ton of OPC produced, approximately 0.7–1 ton of CO_2 is emitted, primarily from the decomposition of calcium carbonate ($CaCO_3$) and the combustion of fossil fuels. These emissions contribute to global climate change, driving the need for sustainable alternatives such as geopolymer

concrete, blended cements, and carbon capture technologies to mitigate the environmental impact of conventional cement production [2]. The production of Ordinary Portland Cement (OPC) demands substantial natural resources, including limestone and significant energy inputs. The extraction and processing of limestone, along with the high-temperature clinkerization process, contribute to resource depletion and environmental degradation. Additionally, concrete made with OPC faces durability challenges that can compromise its long-term performance and structural integrity. One major issue is the corrosion of steel reinforcement, which occurs due to chloride ingress or carbonation, leading to reduced service life and increased maintenance costs. Sulfate attack is another concern, where sulfate ions react with cement hydration products, causing expansion and cracking. Furthermore, OPC-based concrete exhibits limited resistance to high temperatures, leading to strength loss and spalling under fire exposure. Alkali-silica reaction (ASR) between alkalis in cement and reactive silica in aggregates can result in expansive gel formation, causing internal stresses and cracks. Addressing these durability issues remains a significant challenge, necessitating advancements in material design, such as the incorporation of supplementary cementitious materials (SCMs), fiber reinforcement, and alternative binder systems like geopolymer concrete [3]. Also about 40-50% of budget allocated to construction industry is consumed for concrete repair. All the above mentioned issues and problems makes essential for scientists to search for replacements for cementing materials that could reduce the CO_2 emissions to the atmosphere and consequently mitigate the hazards associated with application of Portland cement [5]. In addition, new methods should be developed to use new technologies and novel materials that could lead to more sustainable construction advancements. Scientists have found that alkaline cements are good materials which could maintain the above mentioned conditions and criteria [6]. Alkaline cements are produced by a reaction that takes place between a type of solution from alkaline activators and aluminosilicate materials. The produced matter due to its different forms of reaction could be classified as a gel of either hydrated calcium gel (for systems with high calcium content) or as a 3D aluminosilicate gel (for systems with low calcium content) [7], [8] depending on the chemical composition and structure of used raw materials. The raw materials needed for producing the alkali-activated cements are mainly the by-products of industry such as fly ash and natural pozzolanic materials such as zeolite (Z) and metakaolin (MK) which replace the cement clinker by 100% in activated systems [9]–[12]. Due to these characteristics the alkali-activated cements are often regarded as environmentally friendly materials with a high potential for sustainable development. Among other advantages of concretes made of alkaline cements one could mention reaching a high strength during early ages, increased resistance against fire or chemical attacks [13]–[16]. But most research works that have evaluated thermal stability of concretes activated by alkaline materials have been performed at temperature ranges up to 800 ℃ [5], [17], [18].

In the conventional Portland concrete after reaching this temperature, due to being exposed to fire, the rate of temperature rise slows down and remains constant in the range of 1000-1100℃ which is achieved during a period of 2 or 2.50 hours [19]. Where a structure is continuously exposed to intense fire, concrete shedding and structural damage occur. These phenomena could lead to structural instability of steel structures and even their collapse with increased economic losses or even human fatalities. In this respect, the Portland cement has a major role which could be due to decomposed hydration products within the Portland cement which impact the concrete mechanical properties. In contrast, it is believed that in alkali-activated concretes, due to high temperatures, sintering of the components occurs partially, that causes increased compressive strength in them [20]–[22]. In 2008, Davidovits demonstrated that materials which possess both potassium and sodium in their structure show very good resistance against fire up to 1200℃ temperature [23]. In the another study, Barbosa & Mackenzie in 2003 reached the same results using mixtures that contained activated metakaolin together with sodium hydroxide and sodium silicate [20]. Their findings showed that contraction was caused by water loss at the temperature range of 100-200℃ , but in the temperature range of 250-800℃ no change occurred in dimensions of the samples. Finally, at temperatures higher than 800 ℃ changes were observed in density which occurred due to crystallization of new phases. However, the opinion of present authors is that contraction occurs due to reaching the melting point or it may happen during the viscous flow condition. However they believed that the process stops at the temperature range of 880-900℃. Then the sample retains its stability till reaching temperature range of 1000-1300℃ at which it would melt finally depending on slight changes that occur in its composition. In 2006 another researcher by the name of Bakharev demonstrated that when NA-activated fly ash is subjected to 800℃ temperature, it forms cracks

which are produced due to shrinkage. It also exhibits a slight loss in strength that could be attributed to increased mean pore size and aluminosilicate gel deterioration [18]. In 2015 Martin et al., investigated the behaviour of alkali-activated cements with activated fly ash using a solution containing sodium hydroxide and sodium silicate. They made a comparison between the mentioned cements and the ordinary cement based specimen [22]. Moradikhou et al. used recycled material named coal washing waste in geopolymer concrete to improve post-fire resistance strength. The result presented proper resistance for investigated temperatures so that it is almost stable up to 800 °C [24].

The researchers found that the alkali- activated specimens exhibited increase of strength at temperatures higher than 600℃. This is contrary to what happens with OPC specimens that exhibit loss in mechanical strength properties at this temperature.

Considering the obtained aforementioned results, the objective of this research was performance evaluation of mechanical and post-fire behaviour assessment of binary and ternary eco-friendly Geopolymer Concrete (GPC) containing Autoclaved Aerated Block Waste (AABW) as a fine aggregate. In the next step, Machine Learning (ML) techniques are developed to present an innovative predictive models.

2. Experimental program

2.1. Materials specifications

In this section, the used materials in the experimental program are presented in Figure 1 and detailed in following sentences.

a) SCMs

In this research, the low calcium FA with a granule density of 2.66 g/cm^3 was maintained from Foolad Mobarakeh in Esfahan. In addition, the used Clinoptilolite type of zeolite (Z) for this study was supplied from Semnan mines in Iran, and had a specific gravity of 2.14 and Blaine fineness of 6788 cm^2/g. Moreover, Delijan MK was used as pozzolan which was supplied from the Ferro Alloy Industries Co. having a granule density of 2.59 g/cm^3. The total amount of Al2O3, SiO2, and Fe2O3 in the zeolite was about 80%. This value is higher than the lowest required amount (70%) that is suggested by ASTM C 618 for natural pozzolans. The chemical properties and loss on ignition (LOI) of the used pozzolans are given in Table 1. In the mentioned table due to the rounding of the values, the sum of the percentages of different components is not equal to 100%.

Table 1. Chemical composition of utilized materials (%)

Component (%)	Z	FA	MK
SiO_2	67.79	61.3	52.1
Al_2O_3	13.66	28.8	44.7
Fe_2O_3	1.44	4.98	0.8
CaO	1.68	1.05	0.09
MgO	1.2	0.63	0.03
SO_3	0.5	0.13	-
Na_2O	2.04	0.24	9.1
K_2O	1.42	1.4	0.03
Loss of ignition	10.23	0.7	0.7
Specific gravity	2.3	2.6	2.6
Fineness (m^2/kg)	320	310[a]	12000

b) Alkaline solution

The alkaline solution used in the presented study to activate the SCM (e, g., FA, MK and Z) was a compound of glass water (sodium silicate or Na_2SiO_3) and sodium hydroxide (NaOH). The solid sodium hydroxide 96% was

prepared as a water soluble solution. The sodium silicate solution utilized in this research had a SiO_2 / Na_2O ratio equal to 2.27 (SiO2 = 35.9%, Na_2O = 15.8 %,).

c) Fibers

The experimental investigation for development of eco-friendly GPC mixtures were performed using 2-part hybrid fibers namely steel (St) and polypropylene (PP). Table 2 referred the details of used fibers. The PP fiber length of 6 mm and density of 0.93 was utilized to reinforce the GPC. Moreover, in this study, the hooked-end steel fibers (Length=5, density=7.8 and tensile strength=2500 MPa) having a maximum length equal to 5mm and a diameter equal to 0.12 mm were used to develop and propose the optimal blends. To do so, PP at 0.75, 1, 1.25 vol% and St at 2 vol%, were added in GPC mixture proportions.

d) Aggregates

Autoclaved aerated block waste fine aggregate and Natural Coarse Aggregate (NCA) constituted about 77% of the concrete volume. The autoclaved aerated blocks which used in recycling production for fine aggregate is presented in Fig. 1. The recycled AABW used as fine aggregate was prepared from a local quarry having a fineness modulus equal to 3.05, which was in the recommended range by ASTM C33 [25].

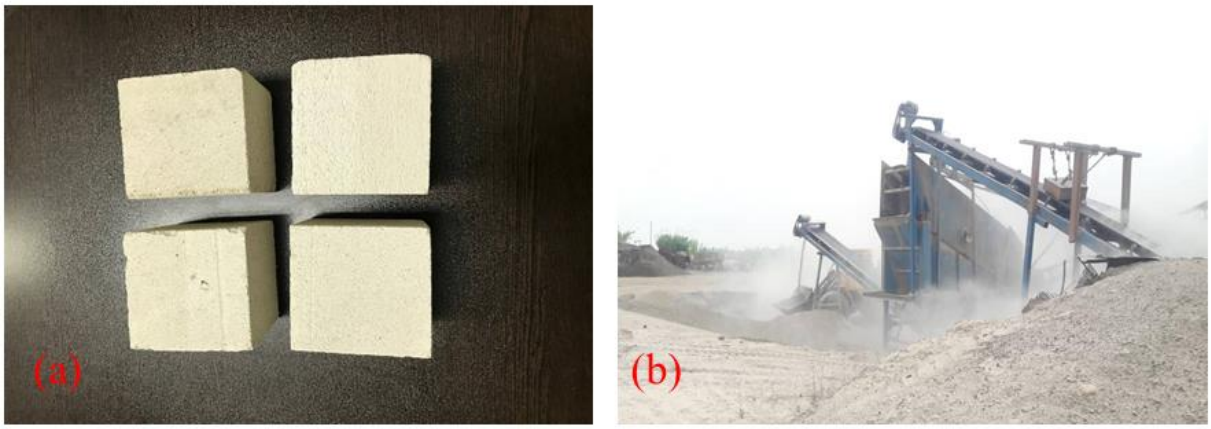

Fig. 1. The AABW aggregate; (a): the autoclaved aerated blocks, (b): recycling process

The used NA had a maximum grain size of 12.5 mm. Also the specific gravity and water absorption values were equal to 2.57 and 1.52%, respectively. Table 2 demonstrates the sieve analyses corresponding to the recycled and fine coarse aggregates.

Table 2. Sieve analysis of coarse and fine aggregates used for GPC mixtures.

NCA	Sieve size (mm)	12.5	8	5.75	4	2	1
	Passing percentage (%)	100	76	47	22	4	2
AABW fine aggregate	Sieve size (mm)	9.5	4.75	2.36	1.18	0.6	0.3
	Passing percentage (%)	100	87.6	63.5	41.9	23.3	4.5

2.2. Mix design, specimen preparation and testing procedure

The mixing of the GPC mixtures containing AABW aggregate was conducted in a mixer. For this aim, dry materials such as AABW, NCA and SCMs were mixed for approximately 3 minutes in the mixer, next the alkaline

solution was added to the mixture and the wet mixing continued for another 4–6 minutes until a consistent mixture was prepared. The fresh mixtures were dumped into steel cube molds with 100×100×100 mm and cylindrical specimens with 100×200 mm. The molds were filled in two layers and each layer was vibrated for about 25 second using a vibrating table. Table 3 presents the mix design GPC mixtures. The Figure 2 is presented the specimen series and their curing condition.

Table 3. Mix proportions of eco-friendly GPC

Series	Sample	SCM			Fiber		NCA (kg/m^3)	AABW (kg/m^3)
		FA (kg/m^3)	Z (%)	MK (%)	Steel (%)	PP (%)		
S0	FAGR0	500	0	0	2	0	500	1036
S1	FAMK10	450	0	10	2	0	500	1036
	FAMK20	400	0	20	2	0	500	1036
S2	FAZ10-MK10	400	10	10	2	0	500	1036
	FAZ10-MK20	350	10	20	2	0	500	1036
	FAZ20-MK10	350	20	10	2	0	500	1036
	FAZ20-MK20	300	20	20	2	0	500	1036
S3	FAGR0-PP0.75	500	0	0	2	0.75	500	1036
	FAMK10-PP0.75	450	0	10	2	0.75	500	1036
	FAMK20-PP0.75	400	0	20	2	0.75	500	1036
	FAZ10-MK10-PP0.75	400	10	10	2	0.75	500	1036
	FAZ10-MK20-PP0.75	350	10	20	2	0.75	500	1036
	FAZ20-MK10-PP0.75	350	20	10	2	0.75	500	1036
	FAZ20-MK20-PP0.75	300	20	20	2	0.75	500	1036
S4	FAGR0-PP1	500	0	0	2	1	500	1036
	FAMK10-PP1	450	0	10	2	1	500	1036
	FAMK20-PP1	400	0	20	2	1	500	1036
	FAZ10-MK10-PP1	400	10	10	2	1	500	1036
	FAZ10-MK20-PP1	350	10	20	2	1	500	1036
	FAZ20-MK10-PP1	350	20	10	2	1	500	1036
	FAZ20-MK20-PP1	300	20	20	2	1	500	1036
S5	FAGR0-PP1.25	500	0	0	2	1.25	500	1036
	FAMK10-PP1.25	450	0	10	2	1.25	500	1036
	FAMK20-PP1.25	400	0	20	2	1.25	500	1036
S6	FAZ10-MK10-PP1.25	400	10	10	2	1.25	500	1036
	FAZ10-MK20-PP1.25	350	10	20	2	1.25	500	1036
	FAZ20-MK10-PP1.25	350	20	10	2	1.25	500	1036
	FAZ20-MK20-PP1.25	300	20	20	2	1.25	500	1036

Figure 2. specimen series

The prepared specimens were kept in the oven at 60 ^{0}C temperature which lasted 24 hours. Then they were removed from the moulds and subsequently cured at the ambient temperature of 24 ± 2 ◦C and the relative humidity of 20% ± 2% to reach the desired temperature according to the ISO-834 standard fire curve and be used for testing. Four cubical shaped specimens and two cylindrical tests for TS and ME were subjected to compression after curing for 28 days based on the requirements of BS EN 12390-3 and ASTM-C496–11, respectively [26]. Also, the ME was evaluated on the 28_{th} day on the cylindrical test according to ASTM-C469–14. For evaluating the post-fire behaviour of the GPC containing AABW aggregate. The specimens were subjected to higher temperatures using a regulated temperature furnace. The furnace was heated at a rate of 10 ◦C/min. When the desired temperature was attained, the temperature was kept fixed for two hours. Then the furnace was cooled at a rate of 1.62 ◦C/min to prevent thermal shocks that might affect the specimens

All of the mixtures had a fixed water-solid materials ratio equal to 0.48. The water consisted of the mixing water and the water that is contained in NaO and Na_2SiO_3. Also the solid materials included FA, MK, Z, and the solid part of the NaOH and Na2SiO3 solutions. Moreover, the sodium hydroxide solution concentrations were 12 Molar; and the Na_2SiO_3 to NaOH ratio was 1/5. For investigating the impact of used SCMs and fibers on the eco-friendly GPC characteristics, 28 mixtures were prepared, where MK and Z were replaced with 0, 10 and 20% FA by weight.

2.3. Overview of ML techniques

a) Multilayer perceptron neural network (MLPNN)

MLPNN are parallel processes with a huge number of neurons (or processing elements) and weighted connections between layers, akin to genuine nervous systems. In the present technique, an MLPNN with three layers comprised of I_j, and k layers and weights W_{ij} and W_{jk} were utilized. A calibration technique was implemented in which the model target variables were compared to the measured outputs. Then the errors were

back-propagated to adjust the randomly assigned initial weights and determine the final weights by minimizing the error [27].
The input x is obtained by weighting the total of the first layer's outputs Next that value is allocated to each neuron of the second and third layers [28]. For example, the y value in the second layer (j), is calculated by the following equation:

$$y_{pj} = \sum_{i=1}^{I} W_{ij} O_{pi} + \theta_j \quad (1)$$

In the above equation θ_j,O_{pi} and W_{ij}, respectively denote the bias for neuron j, the i^{th} output of the first layer, and the weights between the first and second layers. Also to activate y a nonlinear activation function is utilized. The output f(y) is then calculated per each neuron that exists in the second and third layers. Eq. 2 is a logistic function (or common activation function) that is defined as follows:

$$f(y) = \frac{1}{1 + e^{-y}} \quad (2)$$

b) M5 prime

Quinlan proposed his M5 prime tree model by implementing a binary decision tree and using a series of linear regression functions at the leaf (terminal) nodes. [29]–[32]. At the initial phase the standard deviation of class values for a node is taken as error level of the assumed node. Then the projected reduction in error is determined for each attribute [29], [33]. To represent the decrease in errors, the term "Standard Deviation Reduction" (SDR) is employed:

$$SDR = sd(T) - \sum \frac{|T_i|}{T} sd(T_i) \quad (3)$$

In the above equation sd denotes the standard deviation, T_i, denotes the number of samples that represent the i_{th} sample that have the potential rise and T denotes the number of samples. The standard deviation of a child node is smaller than that of the parent node due to the splitting process. Finally the best possible split is selected after analysing all the possible splits in order to minimize the expected error [34]–[36].

3. Results and discussion

3.1. Compressive strength

Figure 3 illustrated the CS evaluation mechanism to define the performances of GPC containing AABW aggregate. For compressive strength, six cube specimens (three specimens are taken for 28-day testing) were tested per each GPC composite according to the ASTM C 39 [37] standard. According to the experimental results which are given in Figure 4, the compressive strength of the GPC changes with the changing contents of the SCMs and their quantity. The compressive strength of GPC containing 10% MK replacement, increased by 9.37% to 38.5 MPa compared with GR0 mix with 35.2 MPa. It rose from 38.5 MPa (by 10% replacement) to 45.8 MPa (by 20% replacement) for MK20, and the maximum compression strength of GPC is observed when 20% of FA is replaced with MK in GPC. By replacing Zeolite with fly ash as the second SCM, it is observed that the compression strength is generally reduced. With increasing amount of Z from 10 to 20 wt.%, compression strength decreased by 14.9% from 36.54 to 31.8 MPa at 28 days with constant content of MK (10 wt.%). This is likely linked to the addition of Z that undermined the system with amorphous phase. This exhibits that it is MK and not Z that greatly helps with increased strength of GPC containing AABW aggregate. It was found that when the MK content increases from 0 to 20%, the corresponding compressive strength increases from about 20 to 80 MPa, respectively.

Figure 3. GPC specimen and testing mechanism

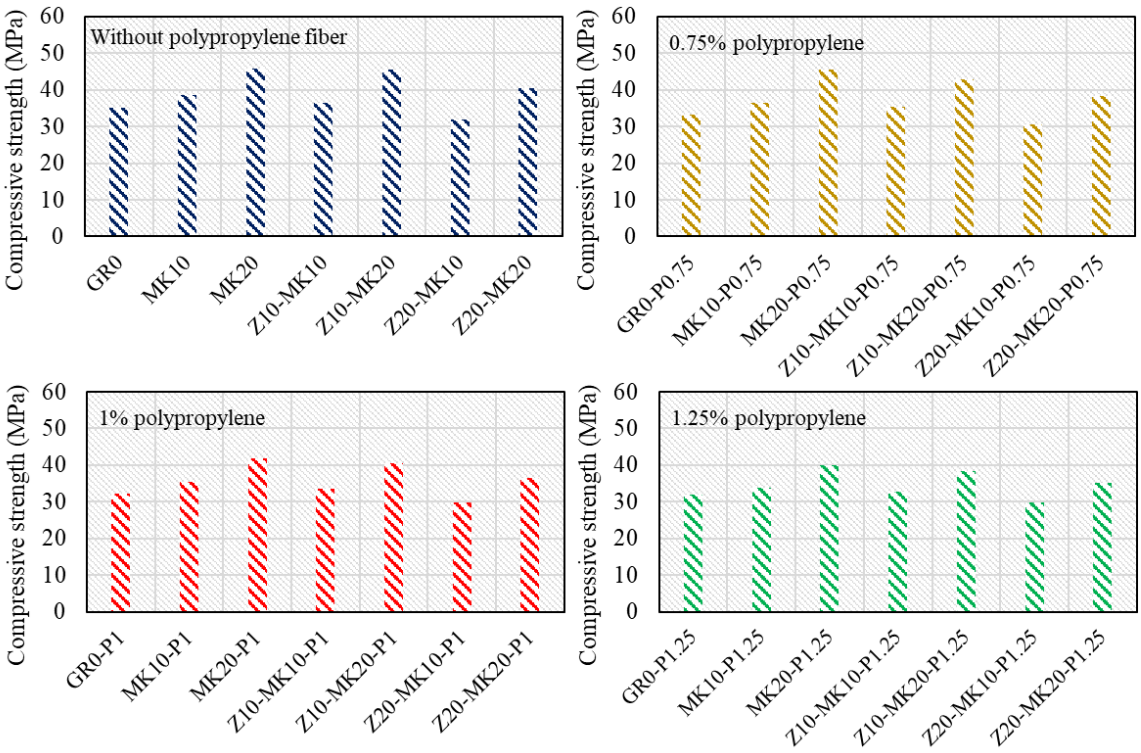

Figure 4. Compressive strength of reinforced AABC-based GPC with different SCMs

Investigating the obtained results for the PP fibre reinforced GPCs (Figure 5), the compressive strength values decrease between 0.9% and 14% in comparison with the control specimen (specimen without PP fibres) when the content of fibres is used for 0.75, 1, and 1.25%. According to the obtained results, it is concluded that the PP fibres generally have a no significant but negative impact on the compressive strength of GPC specimens containing AABW aggregate. The past studies on the impact of PP fibres on GPC compressive strength show inconsistency of the results. In harmony with the above mentioned results, Noushini et al [38] and Moradikhou et al [39] also demonstrated the negative impact of PP fibres on GPC compressive strength and air pocket generation surrounding the fibres. On the other hand, Asrani et al. [40] showed that use of 0.3% volume content PP fibres results in about 6% increase in GPC compressive strength.

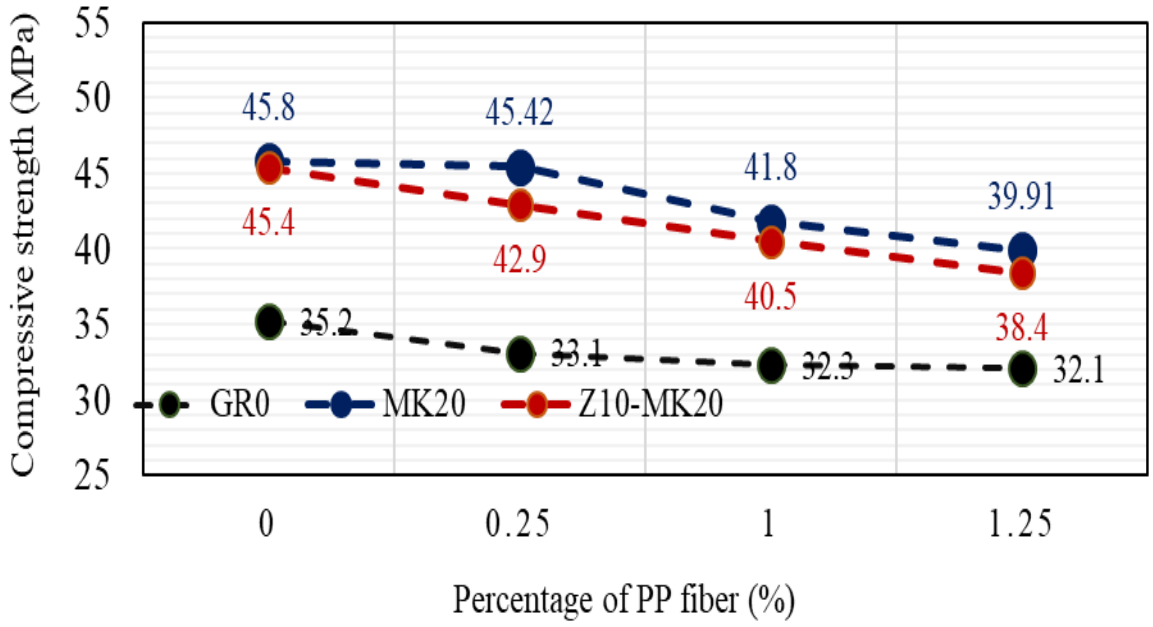

Figure 5. Effect of PP fibers on CS

3.2. Tensile strength

In the Fig. 6, the set up for the tensile strength evaluation which is used in this study was provided. The result of the effects of different proportions of SCMs and PP fibre contents on the tensile strength of GPC at 28 days was indicated in Fig. 7. It was observed that splitting tensile strength increased by about 10% in the case of 10% MK-based GPC specimens cured at the ambient temperature for 28 days compared with the ordinary concrete. Contrary to the compressive strength results, the tensile strength test results showed that increasing the fibre content up to 1.25% enhanced the tensile strength compared to eco-friendly GPC containing AABW aggregate without fibre (which was reported by many scholars). However, presence of fibres has a much stronger impact on the tensile strength in comparison to the compressive strength. For instance, the strength values of MK10 and Z10-MK10 specimens increased by 20.51% and 19.04% from 0.75 volume percent (%) to 1.00 volume percent (%) respectively. The highest strength equal to 5.7 MPa belonged to MK20-P1.25 which corresponded to the highest fibre content (1.25 vol %), which is 1.96 times that of ordinary GPC mixes which lacked PP fibres (2.9 MPa).

Figure 6. Tensile strength set up

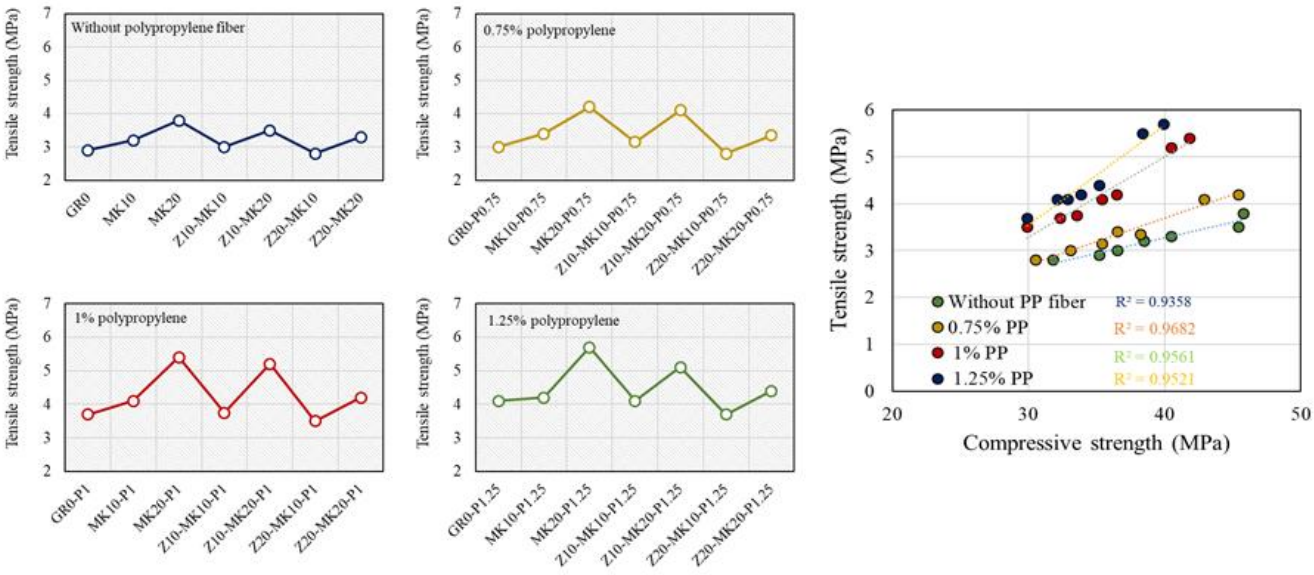

Figure 7. Tensile strength of the eco-friendly GPC with different SCMs

In addition, the strength of concrete that contained MK pozzolan was higher than that with Z pozzolan with the same fibre content (Figure 8). The greatest difference between MK-based GPC specimens was observed at 1.25 vol%. The corresponding tensile strength of MK20-P1.25 at the above mentioned volume percentage was 35.72% higher than that of MK10-P1.25. The results of experimental tests show that by adding Z pozzolanic material 10 and 20% replaced with FA, the tensile strength is generally decreased insofar as it decreased less that plain GPC specimens containing AABW aggregate.

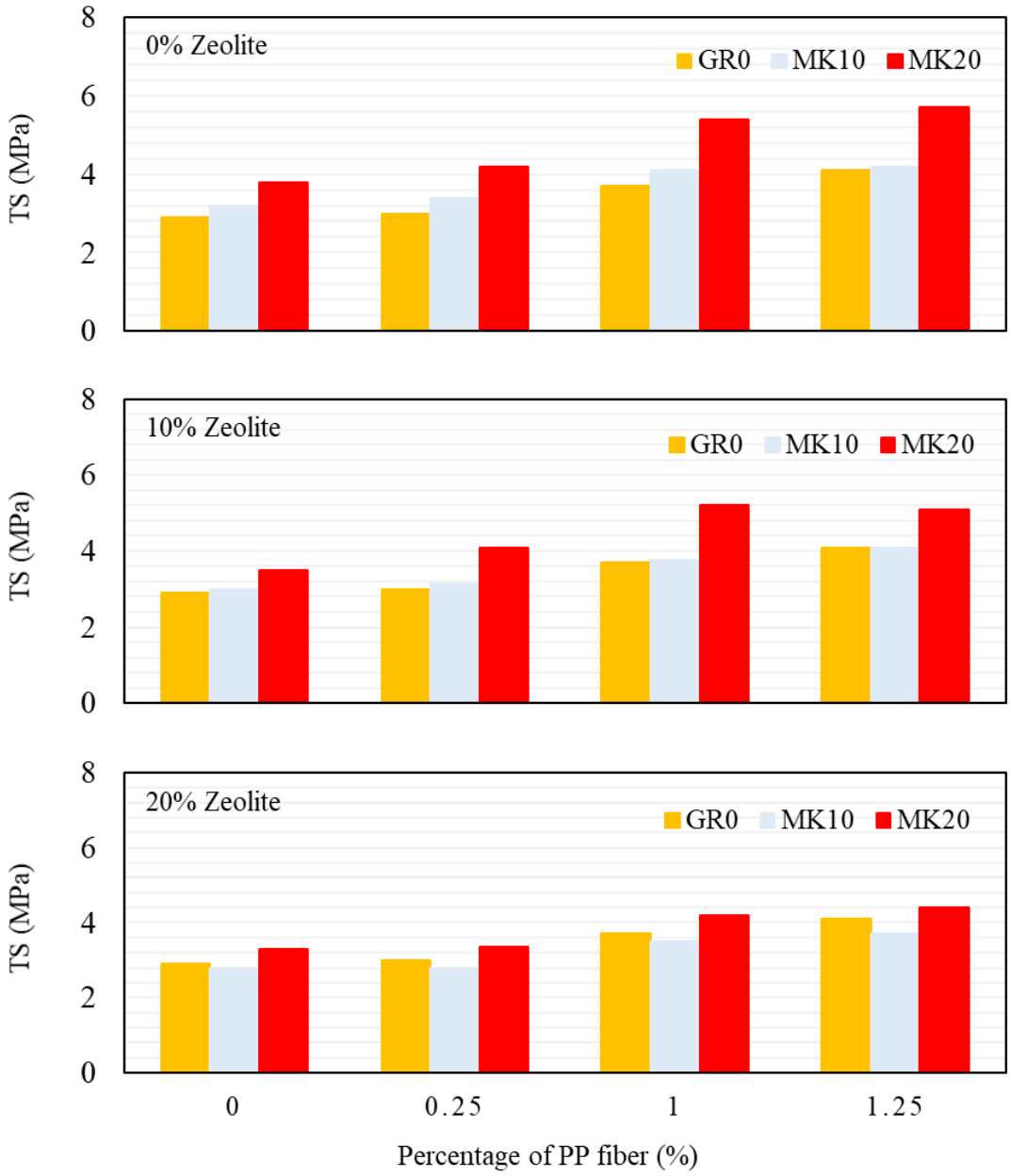

Figure 8. Effect of PP fibers on TS

3.3. Modulus of elasticity

Modulus of elasticity is a mechanical property of concrete that is used in design aspects of structural members, i.e., columns, beams, and slabs. It determines the resistance of concrete members to elastic deformation against the applied load. According to experimental results, similar to compressive strength, modulus of elasticity of GPC specimens experienced insignificant changes with different percentages of PP fibres, ranged from 0 to 1.25 vol%. As Figure 9 shows, the elastic modulus of MK-based FRGPC mixes increased steadily by increasing the MK from 0% to 20%. Whereas, 20% addition MK in FA-based FRGPC showed better results than 10% addition. The modulus of elasticity for the mixes without PP fibres, MK10, MK20, Z10-MK10, Z10-MK20, Z20-MK10, and Z20-MK20 after 28 days of curing were 28.6, 31.14, 27.7, 31.05, 25.95, and 28.95 GPa, respectively with that for the controlled mix is 27.4 GPa. From the results, it can be concluded that the addition of 10 and 20% zeolite reduces elastic modulus values by 3.14 and 9.26% with constant value of MK (i,e., 10% replacment).

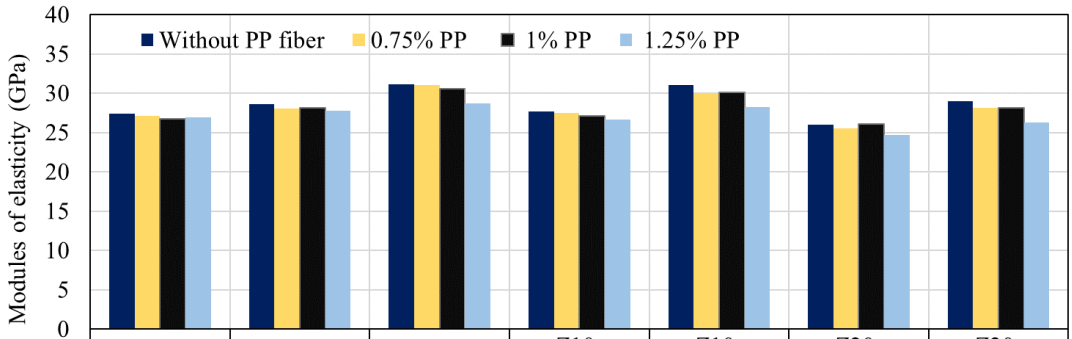

	GR0	MK10	MK20	Z10-MK10	Z10-MK20	Z20-MK10	Z20-MK20
Without PP fiber	27.4	28.6	31.14	27.7	31.05	25.95	28.95
0.75% PP	27.1	28.05	31.05	27.5	30.05	25.5	28.1
1% PP	26.7	28.1	30.6	27.1	30.1	26.1	28.1
1.25% PP	26.9	27.8	28.7	26.6	28.2	24.7	26.3

Figure 9. Elastic modulus of reinforced FRGPC with different SCMs

3.4. Post-fire behaviour evaluation

The images given in Figure 10 show the mixtures with 0.75% PP fibres at ambient temperature and after exposure to 200 ˚C, 500 ˚C, and 800 ˚C. The specimens subjected to 200 ˚C exhibited a slightly reduced opacity with black spots at locations that coincided with the surface voids. In addition, the decolourization of the sample is tending to white and this trend intensifies with increasing temperature up to 800 ˚C. It is noteworthy that, none of the tested specimens at various levels of heat exposure except tor 800 ˚C, experienced visible spalling or corner breakage. Furthermore, a number of major or minor cracks appeared after exposure to 600 ˚C temperature. The lower spalling challenge in eco-friendly GPC at the elevated temperature is facilitated from the highly connected pore structures and lower resistance for degradation with the high temperatures.

Figure 10. GPC samples before and after exposure to elevated temperatures.

Fig. 11 shows the residual compressive strength versus the exposure temperatures of 200 ˚C, 500 ˚C, and 800 ˚C for each 4 levels of PP fibres (i.e., 0, 0.75%, 1%, and 1.25%) in different mixtures. As is seen from the results, the compressive strength of GPC increased first for all mixes but in the range of 400 - 800˚C it decreased at a higher rate. Previously it was demonstrated that the GPC yields a higher strength when it is cured under higher

temperatures. Thus, it is seen that densification of geopolymer occurs at the temperature range of 200-400 ˚C, which leads to increased compressive strength. The particles that contained hydroxyl ions (OH^-) are bound to each other by a dehydration reaction, which causes exit of water and formation of larger particles at 200- 400 ˚C temperature range. The fly-ash-based geopolymer concrete possesses a chemically bonded hydroxyl group to silicon (Si–OH), where at extreme temperatures would form a Si–O–(Si or Al) structure, which could increase its stability and strength [41], [42]. But, when the temperature increases from 400 to 800 ˚C intense cracks with macro scale appear in the specimens. This may be explained in this way that dehydration damage, sintering or dimensional instability could cause damage to the cellular structure of the geopolymer concrete [43], [44].

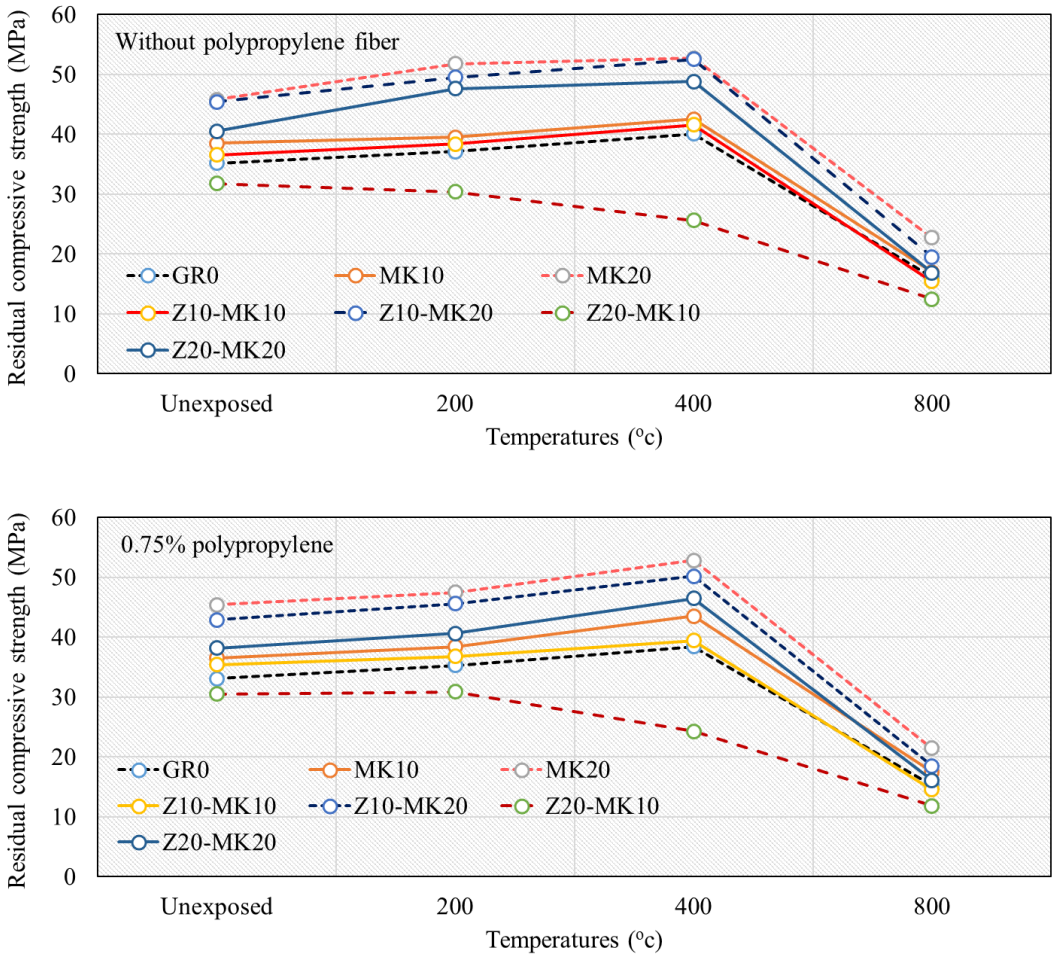

Figure 11. Post-fire evaluation of the GPC mixtures.

It is clear that the higher content of MK in GPC incorporating AABA aggregate caused reduced residual compressive strength and the lower exposure temperature corresponding to peak residual compressive strength. Next by increasing the Z content, the residual compressive strength for each temperature exposure is reduced. The results indicated that by replacing 10% zeolite with metakaolin, the residual compressive strength at 800 ˚C can be reduced by 32.27% compared with 20% metakaolin replacement in the GPC specimens without PP fibres. The Fig. 12 presented the MK20% with 0.75% PP sample before the post-fire evaluation and after the firing at the 200, 500, 800 ^{0}C. According the Fig. 12 at the 400 ^{0}C and 800 ^{0}C, in addition to the cracks and micro cracks, spalling is characterised. The lower spalling challenge in eco-friendly GPC at the elevated temperature is facilitated from the highly connected pore structures and lower resistance for degradation with the high temperatures.

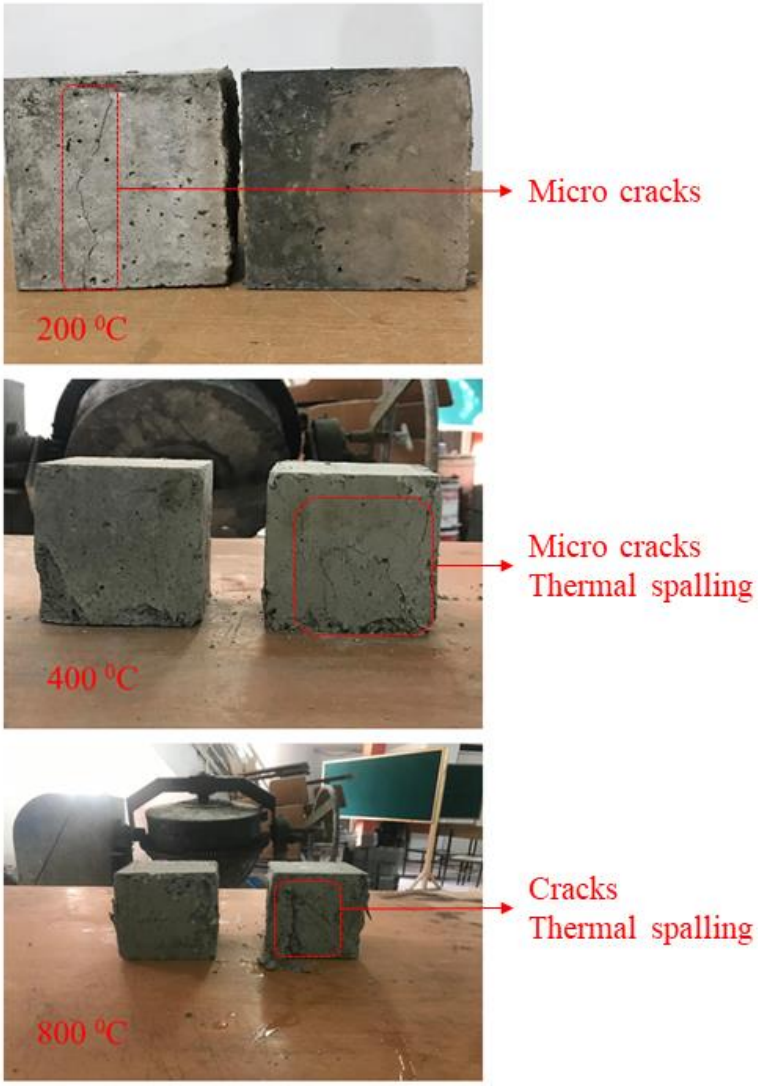

Figure 12. Comparison between the fire resistance behaviour for MK20% with 0.75% PP sample

3.4.1. Micro structure evaluation of post-fired GPC mixture

Scanning electron microscopy (SEM) images were used to evaluate the microstructure of the sample of eco-friendly GPC mixtures containing AABA aggregate at the elevated temperature. To do so, MK20% with 0.75% PP exposed to elevated temperature sample was assessed via SEM analysis. Fig. 13 was presented the micro structure-based SEM evaluation at the 500X, 1000X and 2000 magnification. Based on the presented results, it can be seen that the microstructure of concrete will change when exposed to elevated temperature. According to SEM results, it can be said that the dense and homogeneous structure of aluminosilicate has been preserved at 200 degrees. The FA is rich in calcium and some Al and Ca ions are released during the dissolution process and calcium silicate hydrate (C-A-S-H) nanostructure is formed during the reaction of the alkaline solution. At the temperature of 300 to 700 degrees, there have been many chemical and physical changes in the geopolymer mixtures. At a temperature of 300 ^{0}C, water inside the chemical bond starts to decompose. The dehydration process that started at 100 degrees continues until 200 degrees. This evaporation of water from the geopolymeric structure has caused thermal shrinkage and micro cracks and will cause weight loss of the sample. At a temperature of 500 degrees, OH also evaporates the hydroxyl groups. OH is on the surface and edges of each conductor of geopolymer. In this step, the OH of the hydroxyl group is converted to dihydroxyl and dihydroxylation. Dihydroxylation process affects the compressive strength, weight loss and length changes of the samples. With

the beginning of the dihydroxylation process, the structure of aluminosilicate is changing to calcium carbonate. Also, this structure appears as crystalline or semi-crystalline structures. As the crystal structure increased, micro cracks and holes expanded. In addition, elevated temperature between 500 and 700 degrees causes destruction and formation of new carbonate minerals. By increasing the temperature up to 700 degrees, a stable crystal structure is observed. Also, reduction of crystal structure, increase of cracks and holes on the structure of geopolymer was seen. After decomposition, calcium carbonate turns into calcium oxide and carbon dioxide at temperatures as high as 700 degrees. In fact, when calcium carbonate is decomposed into calcium oxide (lime), the overall structure of the aluminosilicate network changes to a porous and glassy structure. In total, dehydration occurs up to a temperature of 300 degrees and dihydroxylation occurs at around 500 to 700 degrees. Also, heat has destroyed the microstructure of C-A-S-H and C-S-H in geopolymeric mortar. Applying elevated temperature has turned the amorphous aluminosilicate structure of the geopolymer into a ceramic-like structure.

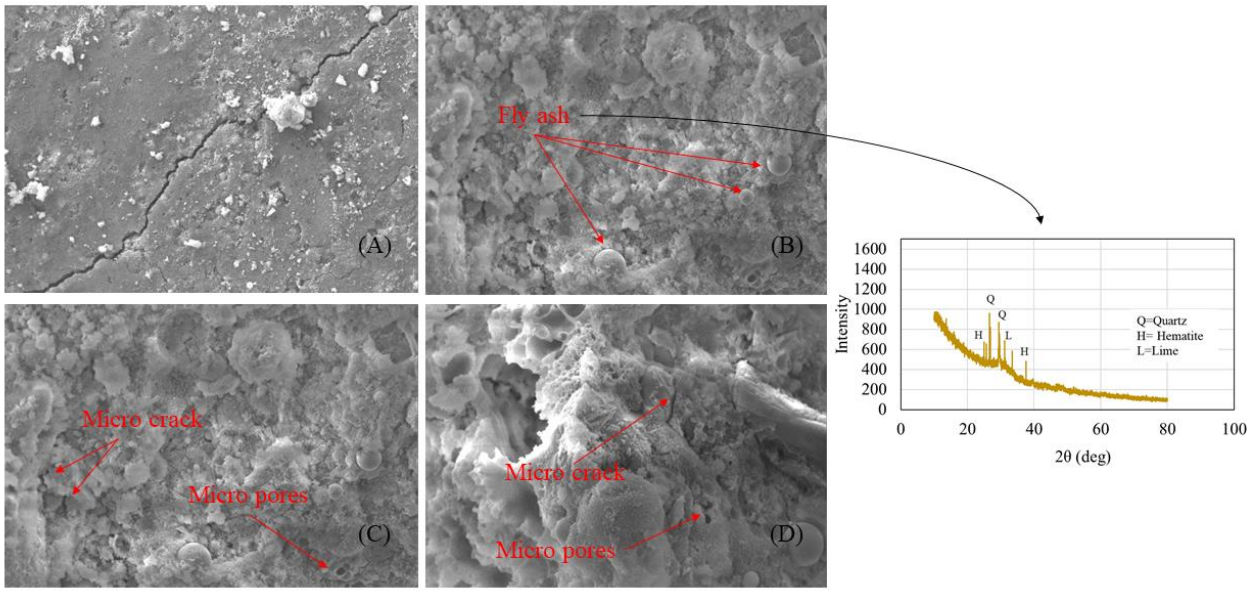

Figure 13. SEM analysis of MK20 sample containing 400 kg/m^3 FA and 20 MK replacement with 0.75% PP; A: 500X with crack detailing, B: 500 X, C: 1000 X, D: 2000 X

3.5. ML-based modelling result and analysis

The results of the proposed MLPNN and M5 prime models to forecast ME, CS, and TS, are given and analysed in this section. It is proven that having a more reliable model largely depends on the used database integrity and providing a large variety of experimental dataset. For this purpose, the experimental results corresponding to the current research and those of the previously published studies [45]–[49] were compiled into a database. One of the important steps for ML-based models development, is selecting appropriate independent variables for simulation of the target variables (i.e., CS, TS, and ME). In preparation of the GPC, various relevant parameters can be considered to obtain the mechanical characteristics of GPC. In this study, the following four parameters incorporating various mix design parameters were considered for developing MLPNN and M5 prime models.

$$CS, TS, and\ ME = f(\%F, AS, AR, B/A) \quad (4)$$

In which, %F, AS, AR, B/A, respectively, are the percentage of total fibre, alkaline solution, aggregate ratio, binder to aggregate ratio. The database contains 181 CS and 106 TS, and 76 ME of test results. The data attributes, units, applied abbreviations, and their changes are given in Table 4.

Table 4. Statistical analysis of independent and dependent variables

Mix Components	Abbreviation	Unit	Range	Mean
Independent variables				
Fiber percentage	%F	(%)	0-3	0.46
Alkaline solution	AS	Kg	135-456	238.38
Aggregate ratio	AR	-	39.93-80.2	70.81
Binder to aggregate ratio	B/A	-	0.186-1	0.276
Dependent variables				
Compressive Strength	CS	MPa	7.62-162.6	39.814
Tensile strength	TS	MPa	0.8-6.9	4.04
Modulus of elasticity	ME	GPa	7-35.2	22.106

In order to perform the ML-based analyses, we divided the database into two groups, randomly: so that 75% (135, 80, and 57 data points were employed for CS, TS and ME, respectively) of the datasets were utilized for the training stage. Then, the remaining datasets (46, 26, and 19 data points were employed for CS, TS and ME, respectively) were used in the validation stage.

In order to evaluate the prediction results of each mechanical property and accuracy of those ML-based models, several performance metrics were calculated and employed including the root mean square error (RMSE), correlation coefficient (R), and mean absolute error (MAE):

$$\boldsymbol{R} = \frac{\sum_{i=1}^{M}(O_i - \bar{O}).(P_i - \bar{P})}{\sqrt{\sum_{i=1}^{M}(O_i - \bar{O})^2 \sum_{i=1}^{M}(P_i - \bar{P})^2}} \quad (5)$$

$$\boldsymbol{RMSE} = \frac{\sum_{i=1}^{M}(P_i - O_i)^2}{M} \quad (6)$$

$$\boldsymbol{MAE} = \frac{\sum_{i=1}^{M}|P_i - O_i|}{M} \quad (7)$$

In the above equations, $\bar{O}$ denotes the mean of O (observed target), $\bar{P}$ denotes the mean of P (predicted target), and M represents the datasets number. In the present study, M5 prime models were utilized for forecasting the CS, TS, and ME of GPC values with hybrid fibres (steel and PP) using 5, 5 and 2 linear models, respectively. The mentioned linear equations are presented in Tables 5-7, based on the rules (conditional sentences). As is seen in the above mentioned tables, the M5 prime rules for CS and ME depend on the binder to aggregate ratio, Also TS depends on the total percentage of fibres.

Table 5. Linear rules of the proposed M5 prime technique for compressive strength

Linear Model	Inputs					Rules of M5 prime
	%F	**AS**	**AR**	**B/A**	**Intercept**	
CS1	+1.933	+0.756	+0.484	+42.052	-143.726	B/A <=0.215
						|AS <=177.45
CS2	+1.933	-0.0385	-0.032	+42.052	+20.92	AS >177.45
CS3	+1.933	+0.756	+0.484	+42.052	-143.726	AR <=61.37:
CS4	-2.48	+0.051	1.283	63.469	-73.755	||AR <=72.245
CS5	-0.077	0.0239	1.483	66.66	-123.397	||AR >72.245

Table 6. Linear rules of the proposed M5 prime technique for tensile strength

Linear Model	Inputs				Rules of M5 prime
	%F	AS	AR	Intercept	
TS1	+0.148	-0.004	-	4.244	%F<=0.125 |AS<=198.25
TS2	+0.148	-0.0006	-	4.71	|AS> 198.25 ||%F<=71.816
TS3	+0.148	0.0075	-	5.443	||AR>71.816 %F>0.125:
TS4	-0.152	-0.001	0.032	3.253	|AS <=254.998
TS5	+0.286	0.012	0.025	-1.539	|AS >254.998

Table 7. Linear rules of the proposed M5 prime technique for modulus of elasticity

Linear Model	Inputs				Rules of M5 prime
	%F	AR	B/A	Intercept	
ME1	+0.002	-1.876	-104.78	+184.041	B/A <=0.872
ME2	0.0017	-0.876	+86.05	+184.041	B/A>0.872

Now, as Table 8 also reveals, there are obvious differences in terms of accuracy and goodness of fitting between MLPNN and M5 prime models in predicting the three mechanical properties of eco-friendly GPC. For the prediction of CS, the M5 prime compared with MLPNN gives higher accuracy and less variance between the actual and predicted outputs. The accuracy of the M5 prime model with respect to the MLPNN model (by calculating the CS, TS and ME of R) is increased by 4.65, 7.9 and 14.9%, respectively. In addition, the minimum values of RMSE and MAE calculated for the M5 prime model correspond to the minimum volatility of fitting dataset and the maximum fitting precision, respectively. The formula extracted from M5 prime strength predictive model predicted the tensile strength with a RMSE value equal to 0.447 MPa. This value shows that the differences between the predicted results and those obtained by experiment are insignificant.

Table 8. Evaluation of predicting CS, TS, and ME characteristics of eco-friendly GPC

Target variable	Method	R	RMSE	MAE
CS (MPa)	MLPNN	0.862	14.519	12.825
	M5 prime	0.907	11.307	8.961
TS (MPa)	MLPNN	0.822	0.587	0.505
	M5 prime	0.887	0.447	0.334
ME (GPa)	MLPNN	0.748	6.137	4.738
	M5 prime	0.863	4.557	3.585

The three estimated properties of GPC by MLPNN models were not much more accurate than those obtained by the M5 prime models. This indicates the poor performance of the other models. The mechanical properties

obtained using the M5 prime model were very close to those obtained by experiments compared with the MLPNN results. This indicates that the M5 prime model was capable of generating accurate mechanical properties that were close to the experimental results. Furthermore, it was found that the MLPNN model could not accurately predict of the GPC properties, since its hyper parameters were tuned by the trial and error procedure.

4. Conclusion

An experimental investigation on the mechanical properties of geopolymer concrete containing SCMs and hybrid steel and polypropylene fibres with various content was carried out in this research. Afterward, two type of machine learning techniques, MLPNN and M5 prime, was implemented to model the mechanical properties of eco-friendly GPC containing Autoclaved Aerated Block Waste (AABW) aggregate. The main results drawn from this study can be summarized as below:

- Fibers slightly decreased the compressive strength of GPC and the 1.25% PP fibres displayed the least performance, i.e. around 13% decrease, compared to the unreinforced GPC containing AABW aggregate. The addition of metakaolin by 20% replacement of fly ash improved the compressive strength of GPC leading to enhancement of amorphous phase content required for the geopolymerization reaction compared with zeolite.
- Presence of PP fibres has a much stronger impact on the tensile strength in comparison to the compressive strength. There was a continuous enhancement in the splitting tensile strength with the increasing content of PP fibres from 0% to 125%, the turning point was found to be at 125% PP fibres content. The results of experimental tests show that by adding Z pozzolanic material 10 and 20% replaced with FA, the splitting tensile strength is generally decreased insofar as it decreased less that plain GPC specimens.
- It is observed that modulus of elasticity of GPC specimens containing AABW aggregate like compressive strength experienced insignificant changes with different percentages of PP fibres, ranged from 0 to 1.25 vol%. In addition, elastic modulus values decreased by 3.14 and 9.26% with 10% constant value of MK since 10 and 20% zeolite was added into the mix design.
- Post-fire behaviour of GPC exhibit that the compressive strength of GPC increased first for all mixes but in the range of 400 - 800°C it decreased at a higher rate due to the dehydration of the geopolymer matrix. Besides, the melting of the fibres due to high temperature and the thermal reaction mechanism of free water evaporation causes the reduction on mechanical properties by a temperature range of 400°C to 800°C.
- By examining the correlation between the target (experimental) values and those predicted by M5 prime, the robustness and potential of the M5 prime for simulating and formulating the strength properties of GPC, compressive strength, tensile strength, and modulus of elasticity, with hybrid steel-PP fibres were established. The results of the ML-modelling, then compared with MLPNN using performance metrics. The accuracy of the M5 prime model with respect to the MLPNN model (by calculating the CS, TS and ME of R) is increased by 4.65, 7.9 and 14.9%, respectively.

References

[1] J. Berry, M., Cross, D., & Stephens, “Changing the environment: an alternative ‘Green’ concrete produced without Portland cement.”.

[2] A. M. Mustafa Al Bakria, H. Kamarudin, M. Bin Hussain, I. Khairul Nizar, Y. Zarina, and A. R. Rafiza, “The Effect of Curing Temperature on Physical and Chemical Properties of Geopolymers,” Phys. Procedia, vol. 22, pp. 286–291, Jan. 2011, doi: 10.1016/J.PHPRO.2011.11.045.

[3] H. AzariJafari, M. J. Taheri Amiri, A. Ashrafian, H. Rasekh, M. J. Barforooshi, and J. Berenjian, “Ternary blended cement: An eco-friendly alternative to improve resistivity of high-performance self-consolidating concrete against elevated temperature,” J. Clean. Prod., vol. 223, no. March, pp. 575–586, 2019, doi: 10.1016/j.jclepro.2019.03.054.

[4] M. Noparast, M. Hematian, A. Ashrafian, M. Javad, T. Amiri, and H. Azarijafari, “Development of a non-dominated sorting genetic algorithm for implementing circular economy strategies in the concrete

industry," Sustain. Prod. Consum., vol. 27, pp. 933–946, 2021, doi: 10.1016/j.spc.2021.02.009.

[5] Z. Pan, J. G. Sanjayan, and B. V Rangan, "An investigation of the mechanisms for strength gain or loss of geopolymer mortar after exposure to elevated temperature," J. Mater. Sci., vol. 44, no. 7, pp. 1873–1880, 2009, doi: 10.1007/s10853-009-3243-z.

[6] A. A. Shahmansouri, H. Akbarzadeh Bengar, and H. AzariJafari, "Life cycle assessment of eco-friendly concrete mixtures incorporating natural zeolite in sulfate-aggressive environment," Constr. Build. Mater., vol. 268, p. 121136, Jan. 2021, doi: 10.1016/j.conbuildmat.2020.121136.

[7] C. A. Rees, J. L. Provis, G. C. Lukey, and J. S. J. van Deventer, "The mechanism of geopolymer gel formation investigated through seeded nucleation," Colloids Surfaces A Physicochem. Eng. Asp., vol. 318, no. 1–3, pp. 97–105, Apr. 2008, doi: 10.1016/J.COLSURFA.2007.12.019.

[8] H. Xu and J. S. J. Van Deventer, "The effect of alkali metals on the formation of geopolymeric gels from alkali-feldspars," Colloids Surfaces A Physicochem. Eng. Asp., vol. 216, no. 1–3, pp. 27–44, Apr. 2003, doi: 10.1016/S0927-7757(02)00499-5.

[9] D. L. Y. Kong, J. G. Sanjayan, and K. Sagoe-Crentsil, "Comparative performance of geopolymers made with metakaolin and fly ash after exposure to elevated temperatures," Cem. Concr. Res., vol. 37, no. 12, pp. 1583–1589, Dec. 2007, doi: 10.1016/J.CEMCONRES.2007.08.021.

[10] P. Duan, C. Yan, W. Zhou, W. Luo, and C. Shen, "An investigation of the microstructure and durability of a fluidized bed fly ash–metakaolin geopolymer after heat and acid exposure," Mater. Des., vol. 74, pp. 125–137, Jun. 2015, doi: 10.1016/J.MATDES.2015.03.009.

[11] H. Y. Zhang, G. H. Qiu, V. Kodur, and Z. S. Yuan, "Spalling behavior of metakaolin-fly ash based geopolymer concrete under elevated temperature exposure," Cem. Concr. Compos., vol. 106, p. 103483, Feb. 2020, doi: 10.1016/J.CEMCONCOMP.2019.103483.

[12] J. Wu, Z. Zhang, Y. Zhang, and D. Li, "Preparation and characterization of ultra-lightweight foamed geopolymer (UFG) based on fly ash-metakaolin blends," Constr. Build. Mater., vol. 168, pp. 771–779, Apr. 2018, doi: 10.1016/J.CONBUILDMAT.2018.02.097.

[13] A. Fernández-Jiménez and A. Palomo, "Composition and microstructure of alkali activated fly ash binder: Effect of the activator," Cem. Concr. Res., vol. 35, no. 10, pp. 1984–1992, Oct. 2005, doi: 10.1016/J.CEMCONRES.2005.03.003.

[14] P. Duan, C. Yan, W. Zhou, and W. Luo, "Thermal Behavior of Portland Cement and Fly Ash–Metakaolin-Based Geopolymer Cement Pastes," Arab. J. Sci. Eng., vol. 40, no. 8, pp. 2261–2269, Aug. 2015, doi: 10.1007/s13369-015-1748-0.

[15] B. B. Jindal, T. Alomayri, A. Hasan, and C. R. Kaze, "Geopolymer concrete with metakaolin for sustainability: a comprehensive review on raw material's properties, synthesis, performance, and potential application," Environ. Sci. Pollut. Res., Jan. 2022, doi: 10.1007/s11356-021-17849-w.

[16] J. Cai, X. Li, J. Tan, and B. Vandevyvere, "Thermal and compressive behaviors of fly ash and metakaolin-based geopolymer," J. Build. Eng., vol. 30, p. 101307, Jul. 2020, doi: 10.1016/J.JOBE.2020.101307.

[17] D. L. Y. Kong and J. G. Sanjayan, "Effect of elevated temperatures on geopolymer paste, mortar and concrete," Cem. Concr. Res., vol. 40, no. 2, pp. 334–339, Feb. 2010, doi: 10.1016/J.CEMCONRES.2009.10.017.

[18] T. Bakharev, "Thermal behaviour of geopolymers prepared using class F fly ash and elevated temperature curing," Cem. Concr. Res., vol. 36, no. 6, pp. 1134–1147, Jun. 2006, doi: 10.1016/J.CEMCONRES.2006.03.022.

[19] F. U. A. Shaikh and V. Vimonsatit, "Compressive strength of fly-ash-based geopolymer concrete at elevated temperatures," Fire Mater., vol. 39, no. 2, pp. 174–188, Mar. 2015, doi: 10.1002/fam.2240.

[20] V. F. F. Barbosa and K. J. D. MacKenzie, "Thermal behaviour of inorganic geopolymers and composites derived from sodium polysialate," Mater. Res. Bull., vol. 38, no. 2, pp. 319–331, Jan. 2003, doi: 10.1016/S0025-5408(02)01022-X.

[21] P. V. Krivenko and G. Y. Kovalchuk, "Directed synthesis of alkaline aluminosilicate minerals in a geocement matrix," J. Mater. Sci., vol. 42, no. 9, pp. 2944–2952, May 2007, doi: 10.1007/s10853-006-0528-3.

[22] A. Martin, J. Y. Pastor, A. Palomo, and A. Fernández Jiménez, "Mechanical behaviour at high temperature

of alkali-activated aluminosilicates (geopolymers)," Constr. Build. Mater., vol. 93, pp. 1188–1196, Sep. 2015, doi: 10.1016/J.CONBUILDMAT.2015.04.044.

[23] J. Davidovits, "Geopolymer Chemistry and Applications.," no. 5-th edition. J. Davidovits.–Saint-Quentin, France (Issue January 2008)..

[24] A. B. Moradikhou, M. Safehian, and E. M. Golafshani, "High-strength geopolymer concrete based on coal washing waste," Constr. Build. Mater., vol. 362, p. 129675, Jan. 2023, doi: 10.1016/J.CONBUILDMAT.2022.129675.

[25] H. Qasrawi, F. Shalabi, and I. Asi, "Use of low CaO unprocessed steel slag in concrete as fine aggregate," Constr. Build. Mater., vol. 23, no. 2, pp. 1118–1125, Feb. 2009, doi: 10.1016/J.CONBUILDMAT.2008.06.003.

[26] 12390-3. Testing hardened concrete. Compressive Strength of Test Specimens, BS EN, "Standard, B. (2009).".

[27] A. A. Shahmansouri, M. Yazdani, S. Ghanbari, H. Akbarzadeh Bengar, A. Jafari, and H. Farrokh Ghatte, "Artificial neural network model to predict the compressive strength of eco-friendly geopolymer concrete incorporating silica fume and natural zeolite," J. Clean. Prod., vol. 279, p. 123697, Jan. 2021, doi: 10.1016/j.jclepro.2020.123697.

[28] M. J. TAHERI AMIRI, A. Ashrafian, F. R. Haghighi, and M. Javaheri Barforooshi, "Prediction of the Compressive Strength of Self-compacting Concrete containing Rice Husk Ash using Data Driven Models," Modares Civ. Eng. J., vol. 19, no. 1, pp. 209–221, 2019, Accessed: Feb. 16, 2022. [Online]. Available: https://mcej.modares.ac.ir/article-16-20432-en.html

[29] G. Quinlan, "Models of subsidence mechanisms in intracratonic basins, and their applicability to North American examples," 1987, Accessed: Aug. 20, 2021. [Online]. Available: https://archives.datapages.com/data/cspg_sp/data/012/012001/463_cspgsp0120463.htm

[30] A. Ashrafian, F. Shokri, M. J. Taheri Amiri, Z. M. Yaseen, and M. Rezaie-Balf, "Compressive strength of Foamed Cellular Lightweight Concrete simulation: New development of hybrid artificial intelligence model," Constr. Build. Mater., vol. 230, p. 117048, Jan. 2020, doi: 10.1016/J.CONBUILDMAT.2019.117048.

[31] M. Nematzadeh, A. A. Shahmansouri, and M. Fakoor, "Post-fire compressive strength of recycled PET aggregate concrete reinforced with steel fibers: Optimization and prediction via RSM and GEP," Constr. Build. Mater., vol. 252, p. 119057, Aug. 2020, doi: 10.1016/j.conbuildmat.2020.119057.

[32] A. Ashrafian, M. J. Taheri Amiri, and farshidreza haghighi, "Modeling the Slump Flow of Self-Compacting Concrete Incorporating Metakaolin Using Soft Computing Techniques," J. Struct. Constr. Eng., vol. 6, no. Issue 2, pp. 5–20, 2019, doi: 10.22065/jsce.2018.90214.1243.

[33] A. Ashrafian et al., "Classification-based regression models for prediction of the mechanical properties of roller-compacted concrete pavement," Appl. Sci., vol. 10, no. 11, pp. 1–22, 2020, doi: 10.3390/app10113707.

[34] A. Behnood, K. P. Verian, and M. Modiri Gharehveran, "Evaluation of the splitting tensile strength in plain and steel fiber-reinforced concrete based on the compressive strength," Constr. Build. Mater., vol. 98, no. January 2018, pp. 519–529, 2015, doi: 10.1016/j.conbuildmat.2015.08.124.

[35] A. Ashrafian, A. A. Shahmansouri, H. Akbarzadeh Bengar, and A. Behnood, "Post-fire behavior evaluation of concrete mixtures containing natural zeolite using a novel metaheuristic-based machine learning method," Arch. Civ. Mech. Eng., vol. 22, no. 2, p. 101, May 2022, doi: 10.1007/s43452-022-00415-7.

[36] A. Ashrafian, E. Panahi, S. Salehi, and M. J. Taheri Amiri, "On the implementation of the interpretable data-intelligence model for designing service life of structural concrete in a marine environment," Ocean Eng., vol. 256, p. 111523, Jul. 2022, doi: 10.1016/J.OCEANENG.2022.111523.

[37] F. Acuña, L., Torre, A. V., Moromi, I., & García, "Uso de las redes neuronales artificiales en el modelado del ensayo de resistencia a compresión de concreto de construcción según la norma ASTM C39/C 39M. Información tecnológica, 25(4), 03-12.".

[38] A. Noushini, A. Castel, J. Aldred, and A. Rawal, "Chloride diffusion resistance and chloride binding capacity of fly ash-based geopolymer concrete," Cem. Concr. Compos., vol. 105, p. 103290, Jan. 2020,

doi: 10.1016/J.CEMCONCOMP.2019.04.006.

[39] A. B. Moradikhou, A. Esparham, and M. Jamshidi Avanaki, "Physical & mechanical properties of fiber reinforced metakaolin-based geopolymer concrete," Constr. Build. Mater., vol. 251, p. 118965, Aug. 2020, doi: 10.1016/J.CONBUILDMAT.2020.118965.

[40] N. P. Asrani et al., "A feasibility of enhancing the impact resistance of hybrid fibrous geopolymer composites: Experiments and modelling," Constr. Build. Mater., vol. 203, pp. 56–68, Apr. 2019, doi: 10.1016/J.CONBUILDMAT.2019.01.072.

[41] M. Lahoti, K. K. Wong, E. H. Yang, and K. H. Tan, "Effects of Si/Al molar ratio on strength endurance and volume stability of metakaolin geopolymers subject to elevated temperature," Ceram. Int., vol. 44, no. 5, pp. 5726–5734, Apr. 2018, doi: 10.1016/J.CERAMINT.2017.12.226.

[42] H. Castillo et al., "Factors Affecting the Compressive Strength of Geopolymers: A Review," Minerals, vol. 11, no. 12, p. 1317, Nov. 2021, doi: 10.3390/min11121317.

[43] K. Somna, C. Jaturapitakkul, P. Kajitvichyanukul, and P. Chindaprasirt, "NaOH-activated ground fly ash geopolymer cured at ambient temperature," Fuel, vol. 90, no. 6, pp. 2118–2124, Jun. 2011, doi: 10.1016/j.fuel.2011.01.018.

[44] E. A. Azimi et al., "Strength Development and Elemental Distribution of Dolomite/Fly Ash Geopolymer Composite under Elevated Temperature," Materials (Basel)., vol. 13, no. 4, p. 1015, Feb. 2020, doi: 10.3390/ma13041015.

[45] Y. Chi, M. Yu, L. Huang, and L. Xu, "Finite element modeling of steel-polypropylene hybrid fiber reinforced concrete using modified concrete damaged plasticity," Eng. Struct., vol. 148, pp. 23–35, Oct. 2017, doi: 10.1016/J.ENGSTRUCT.2017.06.039.

[46] Ł. Sadowski, M. Piechówka-Mielnik, T. Widziszowski, A. Gardynik, and S. Mackiewicz, "Hybrid ultrasonic-neural prediction of the compressive strength of environmentally friendly concrete screeds with high volume of waste quartz mineral dust," J. Clean. Prod., vol. 221, pp. 727–740, 2019, doi: 10.1016/j.jclepro.2018.12.059.

[47] X. Yuan et al., "Machine Learning Prediction Models to Evaluate the Strength of Recycled Aggregate Concrete," Materials (Basel)., vol. 15, no. 8, p. 2823, Apr. 2022, doi: 10.3390/ma15082823.

[48] U. S. Biswal, M. Mishra, M. K. Singh, and D. Pasla, "Experimental investigation and comparative machine learning prediction of the compressive strength of recycled aggregate concrete incorporated with fly ash, GGBS, and metakaolin," Innov. Infrastruct. Solut., vol. 7, no. 4, p. 242, Aug. 2022, doi: 10.1007/s41062-022-00844-6.

[49] A. Ahmad, K. Chaiyasarn, F. Farooq, W. Ahmad, S. Suparp, and F. Aslam, "Compressive Strength Prediction via Gene Expression Programming (GEP) and Artificial Neural Network (ANN) for Concrete Containing RCA," Buildings, vol. 11, no. 8, p. 324, Jul. 2021, doi: 10.3390/buildings11080324.